ACS APPLIED MATERIALS & INTERFACES

Research Article

www.acsami.org

Thermal Conductivity and Combustion Properties of Wheat Gluten Foams

Thomas O. J. Blomfeldt,[†] Fritjof Nilsson,[†] Tim Holgate,[‡] Jianxiao Xu,[‡] Eva Johansson,[§] and Mikael S. Hedenqvist*[,†]

[†]Department of Fibre and Polymer Technology, KTH Royal Institute of Technology, SE-10044, Stockholm, Sweden

[‡]Risø National Laboratory for Sustainable Energy, Technical University of Denmark, DK-4000 Roskilde, Denmark

[§]Department of Agrosystems, The Swedish University of Agricultural Sciences, SE-23053, Alnarp, Sweden

ABSTRACT: Freeze-dried wheat gluten foams were evaluated with respect to their thermal and fire-retardant properties, which are important for insulation applications. The thermal properties were assessed by differential scanning calorimetry, the laser flash method and a hot plate method. The unplasticised foam showed a similar specific heat capacity, a lower thermal diffusivity and a slightly higher thermal conductivity than conventional rigid polystyrene and polyurethane insulation foams. Interestingly, the thermal conductivity was similar to that of closed cell polyethylene and glass-wool insulation materials. Cone calorimetry showed that, compared to a polyurethane foam, both unplasticised and glycerol-plasticised foams had a significantly longer time to ignition, a lower effective heat of combustion and a higher char content. Overall, the unplasticised foam showed better fire-proof properties than the plasticized foam. The UL 94 test revealed that the unplasticised foam did not drip (form droplets of low viscous material) and, although the burning times varied, self-extinguished after flame removal. To conclude both the insulation and fire-retardant properties were very promising for the wheat gluten foam.

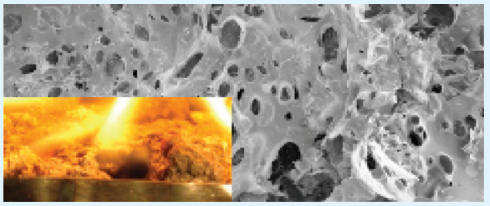

KEYWORDS: *wheat gluten, foam, glycerol, freeze-drying, thermal conductivity, combustion*

INTRODUCTION

Polymer foams are used in a wide range of applications, including sound and thermal insulation.[1] They are generally divided into open- and closed-cell foams.[1] Closed-cell foams are used as building insulation due to their low thermal conductivity. These foams have the lowest thermal conductivity of any conventional nonvacuum insulator,[2] with values below λ = 0.04 W/(m °C).[1] The principal parameters used to describe the heat transport are the thermal conductivity (λ) and the thermal diffusivity (D), which may be calculated from each other, if the specific heat capacity (c_p) and the foam density (ρ) are known[3]

$$\lambda = Dc_p\rho \quad (1)$$

The thermal conductivity of a foam can approximately be expressed as the sum of four separate components[2,4]

$$\lambda = \lambda_s + \lambda_g + \lambda_c + \lambda_r \quad (2)$$

where λ_s is the heat conductivity through the solid phase, λ_g is the heat conductivity through the gas phase, λ_c is the heat convection in the gas phase and λ_r is the radiation through the foam cells.[2,4] It is here assumed that the four contributions occur in parallel. In the case of small cell sizes, convection is limited and radiation reduced (being absorbed, scattered and reflected in the cell walls). With a low conductivity gas and polymer matrix, it is possible to achieve a very low thermal conductivity.[2]

Conventional polymeric foams are prepared from petroleum-based polymers, making them less suitable as environmentally sustainable materials because they contribute to greenhouse gases in the atmosphere and are difficult to dispose of or recycle.[5] Synthetic polymeric foams are intrinsically highly flammable and have a high potential for fire growth due to their low heat capacity, low thermal conductivity and high internal surface area.[6] It has been observed with upholstered furniture that synthetic open foams can have a high flame-spread rate, and this is a major cause of fire-related deaths in the United States.[7] Hence, there is a need for alternative, less flammable foam materials that are made from more renewable resources.

Previous studies have shown that foams can be prepared from wheat gluten using lyophilization (freeze-drying), a technique based on the sublimation of ice, without the need for a "synthetic" blowing agent.[8] Different properties and cell structures were obtained using different concentrations of wheat gluten and/or by adding different amounts of a plasticiser (glycerol) or bacterial cellulose (BC) nanofibers.[8,9] Wheat gluten is a cheap, readily available byproduct from the European ethanol (biofuel) industry[10] with interesting foam-forming properties (high elasticity and good gas barrier properties in dry environments).[10,11]

Received: December 16, 2011
Accepted: February 14, 2012
Published: February 14, 2012

   dx.doi.org/10.1021/am2017877 | *ACS Appl. Mater. Interfaces* 2012, 4, 1629–1635

The aim of the present study was to investigate the thermal insulating and flame-retardant properties of wheat gluten foams in order to evaluate their potential for use as insulation materials. Indeed they showed very promising properties. This is, to the best of our knowledge, the first study of the combustion behavior of a protein-based foam.

EXPERIMENTAL SECTION

Materials. The commercial wheat gluten powder was kindly supplied by Lantmännen Reppe AB, Sweden. According to the supplier, the gluten protein content was 77.7% (w/w) of the dry weight (modified NMKL Nr 6, Kjeltec, Nx5.7, www.NMKL.org), the moisture content was 6.9% (w/w) of the total weight (NMKL 23, 1991), and the starch content was 5.8% (w/w) of the dry weight (Ewers polarimetric method). The fat content was 1.2% (w/w) of the dry weight, (Soxtec, Lidfett.OA.19, tecator AN 301), and the residual ash was 0.9% (w/w) of the dry weight (NMKL 173 seconded). Glycerol (99.5%) was obtained from KarlshamnTefac AB, Sweden.

Foam Preparation. Two types of foam samples were prepared: an unplasticized wheat gluten foam (WG) and a wheat gluten foam plasticized with glycerol (WGG). WG was made by dispersing/mixing 20 g (14 wt.%) gluten in 120 mL distilled water using a Philips Chopper mixer (model HR 1392). The pH was adjusted to pH 11 with sodium hydroxide (NaOH). WGG was prepared in a similar manner but with the addition of 5 g of glycerol (20 wt.% of the gluten/glycerol mixture). When the gluten-based mixture appeared to be uniform, it was heated to 75 °C while undergoing further mixing in a Yellow Line Di 25 basic homogenizer from IKA (model 31 300 00) with the dispersion tool S25N-18G, IKA (model 05 934 00). The mixture was thereafter placed into either parallelepiped-shaped silicone molds (size: 10 × 10 × 14 mm^3), rectangular-shaped silicone molds (50 × 20 × 4 mm^3), larger silicone molds for cone calorimetry measurements (size: 90 × 85 × 20 mm^3), 100 μL aluminum pans (for differential scanning calorimetry) or 70 μL alumina pans (for thermogravimetric analysis). The mixtures were frozen at −25 °C for at least 12 h and then freeze-dried for 24 h (48 h for the large combustion samples) in a 20 × 20 × 4 cm^3 poly(methyl methacrylate) (PMMA) form connected to a Lyovac GT 2 freeze-dryer, GEA Process Engineering Inc. The foams were stored in desiccators over silica gel until measurement or conditioning.

The recipes chosen were based on findings from previous work.[8,9] The use of 14 wt % gluten in water yielded a foam with attractive mechanical properties and a more homogeneous cell structure with a higher content of closed cells than the foam with a lower gluten content. The addition of 20 wt % glycerol was shown previously to lead to sufficient plasticization while having a small effect on the cell structure.[9]

Differential Scanning Calorimetry (DSC). The specific heat capacity (c_p) was determined in an inert atmosphere (50 mL/min N_2) with a Mettler Toledo DSC 1. In the first step the specimen was heated from 25 to 120 °C at a heating rate of 10 °C/min and then held at 120 °C for 5 min. After being cooled to 25 °C (10 °C/min), the specimen was heated a second time from 25 to 80 °C at a heating rate of 2 °C/min. The value of c_p was determined from the second heating to avoid any contribution from nonreversible processes (including the protein denaturation observed in the first heating). The c_p value was estimated by comparing the differences in heat flow rate between an empty and a full sample pan with a foam weight of 14 ± 1 mg (100 μL aluminum pans), according to the following equation

$$c_p = \frac{\Delta Q}{mv} \tag{3}$$

where ΔQ (mW) is the difference in heat flux between the specimen-containing and the empty pan, m (mg) is the specimen mass, and v (°C/s) is the heating rate.

Laser Flash (LF) Method. The thermal diffusivity (D) of the WG foam was determined at 10 °C steps between 30 and 60 °C using a Netzsch LFA 457 laser flash apparatus. A detailed description of the technique and instrument can be found in ref 13. The parallelepiped-shaped samples were cut horizontally into shapes of 10 × 10 × 2−4 mm^3 from the middle section of the specimen using a diamond saw. The samples were thereafter spray-coated with a thin layer of graphite to facilitate the absorption of the laser at the surface of the sample. Three WG replicates were used.

Hot Plate (HP) Method. The thermal diffusivity and conductivity were estimated using an alternative method to the laser flash technique. Cylindrical WG specimens (diameter: 25 mm), conditioned at 23 °C and 50% RH for at least a week, were placed in the same climate room on a plate (central part of an IKA C-MAG HS7 hot plate stirrer (IKA werke GmbH, Germany)) heated to 40, 50, and 60 °C. A solid PMMA (ρ = 1160 kg/m^3) cylindrical sample (diameter: 30 mm and height: 12 mm) was also tested. The specimen temperature was measured on the upper surface using a Testo mini surface thermometer (art. nr. 0900 0619, Testo Ltd.). The planar circular shaped thermometer head covered ca. 30% of the upper surface. D and λ were obtained by fitting the temperature−time data at the upper surface using a finite element model (FEM, calculations made in Comsol Multiphysics and Mathworks Matlab). Mathematically the FEM model was described by combining eq 1 with the heat equation

$$\frac{\partial T}{\partial t} = \nabla(D\nabla T) \tag{4}$$

where T is temperature and t is time. It was here assumed that the contact between the bottom part of the specimen and the plate, as well as between the upper part of the specimen and the thermometer, was good. The boundary condition where the thermometer was in contact with the specimen was based on continuity:

$$\hat{N}(\lambda_1\nabla T_1 - \lambda_2\nabla T_2) = 0 \tag{5}$$

where λ_1 and λ_2 are the thermal conductivities of the foam and the stainless steel thermometer head, the latter taken from the Comsol Multiphysics material library (λ_2 = 13.35 W/(m °C) at 27 °C), and T_1 and T_2 are the corresponding surface temperatures. The boundary conditions of the remaining surfaces were defined such that the flux in the direction normal to the surface ($\hat{N}$) was proportional to the temperature difference between the ambient temperature T_0 (23 °C) and the surface temperature T of the specimen

$$\hat{N}(\lambda\nabla T) = h(T_0 - T) \tag{6}$$

Thermogravimetry (TGA). The WG and WGG foams were studied using a Mettler Toledo TGA/DSC 1 thermogravimeter. All samples were conditioned for 72 h at 23 °C and 50% RH before testing. The samples were heated under a constant airflow of 50 mL/min at a heat rate of 10 °C/min from 25 to 800 °C. Three replicates were used.

Cone Calorimetry. The cone calorimeter experiments were performed on a custom-built apparatus at SP Trätek Wood Technology (Stockholm, Sweden). Calibration was performed as described in ISO 5660−1.[14] WG and WGG foams with densities of 131 ± 6 kg/m^3 and 140 ± 9 kg/m^3, respectively, were used. Samples were conditioned at 50% RH at 25 °C for 1 week before testing. Samples were tested without a retainer frame and with the bottom and the sides of the sample covered with a 35 μm thick aluminum foil. The distance from the cone heater to the sample surface was 25 mm and the incident heat flux was 35 kW/m^2. Three replicates were used.

UL 94 Test. WG was subjected to a flammability test according to UL 94 with some modifications regarding specimen dimensions. Five specimens, with dimensions of 50 × 20 × 4 mm^3, were used. The specimen was clamped with the longitudinal axis in the vertical orientation, so that the lower end of the specimen was ca. 300 mm above a horizontal layer of cotton. The flame of the Bunsen burner was ca. 20 mm high and it was placed ca. 10 mm below the sample for two 10 s periods. During these periods, the burner was placed at an angle of 45° with respect to the vertical position. The time of burning with flaming combustion was measured after the first (t_1) and second (t_2) removals of the Bunsen burner.

Field-Emission Scanning Electron Microscopy (FE-SEM). The ashes of the cone calorimetry-tested foams were examined with a

Hitachi S-4800 FE-SEM. The foam sample surfaces were coated with gold to a thickness of 6 nm using an Agar high resolution sputter coater (model 208RH), equipped with a gold target and thickness monitor.

RESULTS AND DISCUSSION

For convenience, properties of the two foams determined previously are given in Table 1. Compared to WG, WGG had a higher density, larger pore size and higher solids content and showed a higher strain recovery, whereas WG was significantly stiffer. Compared to conventional rigid polyurethane[15] and polystyrene[16] foams for insulation purposes, both WG and WGG foams had a higher density, smaller pores, lower porosity,and a higher volume fraction of open pores.[8]

Table 1. Foam Characteristics[a]

sample	foam density[b] (kg/m^3)	solid content[c] (%)	Young's modulus[d] (kPa)	strain recovery[e] (%)	pore sizes[f] (μm)
WG	134−139	15 ± 0.2	2 300 ± 900	31 ± 4	35−45
WGG	169−182	17 ± 0.2	200 ± 30	94 ± 3	35−60

[a] ± values are standard deviations. [b]Foam density (ρ) obtained from refs 8 and 9. [c]Residual solids content after freeze-drying.[8] [d]Young's modulus obtained in compression according to ISO 844;2007.[9] [e]Strain recovery calculated 72 h after the foam had been subjected to a strain of 80%.[9] [f]Pore sizes obtained by mercury intrusion porosimetry.[8]

The c_p values are plotted in Figure 1 as a function of temperature for WG and PMMA, the latter being studied to assess the validity of the method used. The c_p was found to increase with temperature, in agreement with literature data on foams and solid polymers.[13,17] The specific heat capacity values of PMMA were comparable to those reported elsewhere.[18] The values for WG were of the order of 1.2−1.8 J/(g °C) in the actual interval. Specific heat capacities, under ambient conditions, of polystyrene and polyurethane foams are, respectively, 1.3 and 1.5 J/(g °C).[19]

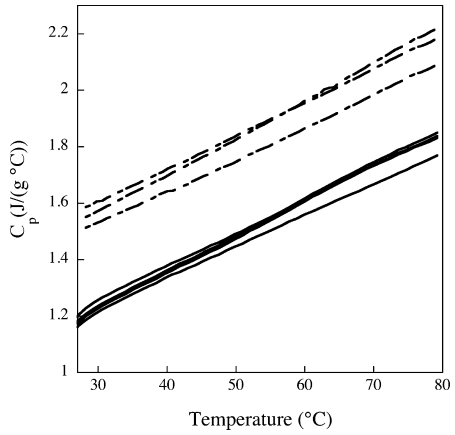

Figure 1. c_p values plotted against temperature for the WG foam (solid lines (4 replicates)) and the PMMA sample (broken lines (three replicates)).

The observed IR detector signal (voltage vs time) in the laser flash measurements could be described by two events: 1) at the instant when the laser pulse was sent there was a narrow peak with a width of the order of a few milliseconds, 2) subsequently, a relatively slow rise, saturation, and possible decay attributed to the rise of the upper surface temperature (opposite of pulse absorption), which together lasted ca. 30 to 60 s. The first event was considered to be a result of the detector "seeing" the pulse flash as some infrared light was scattered throughout the system. The second event was considered to be due to heat conduction in the gas and solid phase of the sample. The time to reach half the IR signal maximum ($t_{0.5}$, eq 7) in the second feature of the curve was used to calculate the thermal diffusivity (L is the sample thickness).[20]

$$D = 0.1388L^2/t_{0.5} \quad (7)$$

The thermal diffusivity data are presented in Table 2. The values were consistently lower than 0.3 mm^2/s, which was lower than the values reported for polyethylene,[3] polystyrene[19] and polyurethane foams.[19,21] This agrees with the fact that the thermal diffusivity normally decreases with increasing density, because of the higher diffusivity of the air/gas. A solid polyethylene sample, with a density of 910 kg/m^3, has a thermal diffusivity of 0.17 mm^2/s, whereas the corresponding foam, density = 31 kg/m^3, has a thermal diffusivity of 0.70 mm^2/s.[3]

Table 2. Specific Heat Capacity, Thermal Diffusivity, and Thermal Conductivity of the WG Foam

method[a]	T[b] (°C)	c_p[c] (J/(g °C))	D[d] (mm^2/s)	λ[e] (W/(m °C))
LF	30	1.24 ± 0.02	0.244 ± 0.015	0.039 ± 0.003
LF	40	1.37 ± 0.02	0.228 ± 0.004	0.041 ± 0.001
LF	50	1.48 ± 0.02	0.225 ± 0.005	0.043 ± 0.002
LF	60	1.59 ± 0.03	0.226 ± 0.002	0.047 ± 0.001
HP$_s$	40	1.37 ± 0.02	0.249 ± 0.009	0.040 ± 0.002
HP$_s$	50	1.48 ± 0.02	0.270 ± 0.021	0.048 ± 0.004
HP$_l$	50	1.48 ± 0.02	0.332 ± 0.024	0.069 ± 0.005
HP$_l$	60	1.59 ± 0.03	0.373 ± 0.023	0.083 ± 0.006

[a]Method used to obtain the thermal diffusivity: LF is the laser flash method and HP is the hot plate method. Indices s and l refer to, respectively, a "short" cylinder with a height of ca. 4.8 mm and a tall cylinder with a height of ca. 7.0 mm. [b]T is the oven temperature in the case of the LF method and the plate temperature in the case of the HP method. [c]Specific heat capacity obtained as an average at the respective temperature from the c_p−T curve in Figure 1. [d]Thermal diffusivity [e]Thermal conductivity calculated according to eq 1. The density used was 130 kg/m^3 for all of the calculations. The maximum and minimum values of λ were estimated by inserting pairwise minimum and maximum values of D and c_p in eq 1.

The thermal diffusivities, obtained by the hot plate method, are also given in Table 2. It should be noted that the temperature given in Table 2 refers to the specimen temperature in the LF experiment and to the plate temperature in the hot plate experiment. Because the experiment in the latter method was conducted under a transient temperature gradient, the average specimen temperature was lower than the value given in Table 2. Nevertheless, since the temperature dependence of the thermal diffusivity was small, it was still possible to compare the values of D obtained by the two methods. The D values obtained on the short specimens were similar to those obtained by the LF method, but the D values obtained on the tall specimens were somewhat higher. This may be explained by considering Figure 2. Figure 2a shows that the increase in temperature at the upper specimen surface can be well described by a "single-stage" process for the PMMA specimen. However, for the foam, there seemed to be a "two-stage" process, which was clearly distinguishable for the tall specimen (Figure 2b); a rapid initial increase followed by a slow

dx.doi.org/10.1021/am2017877 | ACS Appl. Mater. Interfaces 2012, 4, 1629−1635

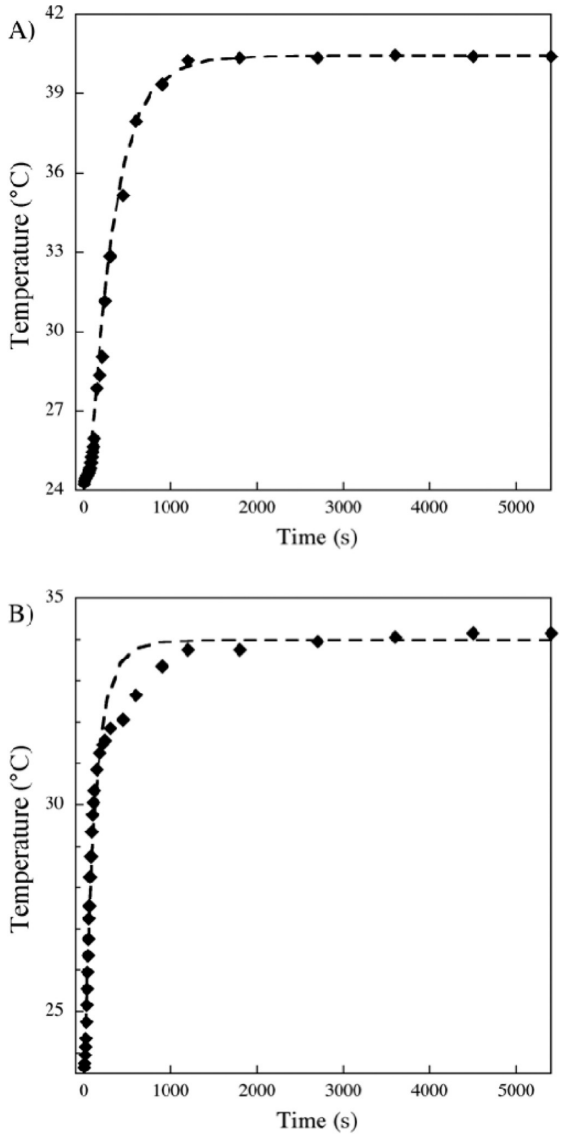

Figure 2. Experimental (♦) and modeled (broken line) upper surface temperature in contact with the thermometer, as a function of time, for (a) a PMMA specimen and (b) a tall WG foam using a 60 °C plate temperature.

increase to the final steady-state temperature. A hypothesis is that the rapid and slow processes were associated with heat transfer in, respectively, the pore and the matrix components. In the calculation of the thermal diffusivity from the "two-stage" curve (Figure 2b), only the first part of the curve was considered, which led to an overestimation of D (Table 2). In the case of the short specimen, there was no overestimation because the two processes seemed to coincide giving a "single-stage" curve, similar to the curve in Figure 2a, that could be fitted completely (not shown). It should be noted that the calculated PMMA thermal diffusivity (60 °C plate temperature) was 0.085 mm^2/s, which was relatively close to a reported value of ~1 mm^2/s.[22]

Table 2 also presents the thermal conductivity values obtained from both the LF and HP methods. In calculating the thermal conductivity with eq 1, it was assumed that the density was temperature-independent and the ambient value was used. The values were, in general, relatively low (0.04–0.05 W/(m °C)), with the exception of those for the tall sample. This was, however, explained by the overestimated diffusivity values (Table 2, Figure 2b). The values were comparable to those of closed-cell polyethylene foams[3] and slightly higher than those of rigid closed-cell polyurethane[21] and polystyrene[19] insulation foams. An interesting finding is that casein/clay composite foams produced by the freeze-drying method, with densities similar to our foams, have a similar thermal conductivity 0.045 W/(m °C).[23]

In order to verify the reliability of the thermal conductivity values obtained with the hot plate method, experimental and literature values of PMMA were compared. The calculated PMMA thermal conductivity using the c_p data in Figure 1, a density of 1160 kg/m^3 and the value of D given above, was ca. 0.19 W/(m °C), which was in agreement with data reported by Assael et al.[24] (0.19–0.20 at 35–60 °C).

The TGA curves for WG (ρ = 126 ± 10 kg/m^3) and WGG (ρ = 145 ± 6 kg/m^3) are presented in Figure 3. In the first

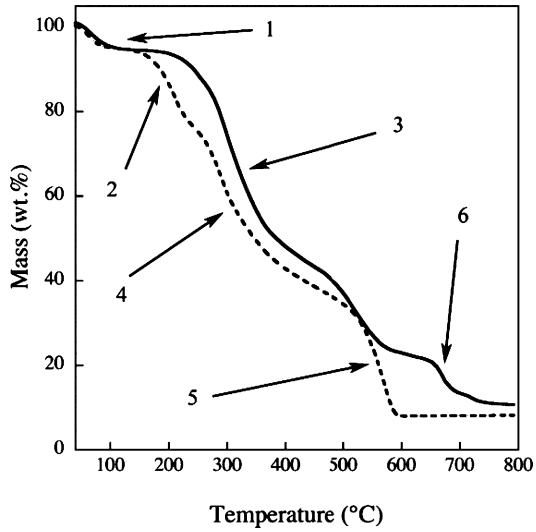

Figure 3. Thermogravimetric curves of the WG (solid line) and the WGG (broken line) foams. The curves are averages of three replicates. Arrows indicate the regions discussed in the text.

region, moisture was evaporating (ending below ca. 120 °C, indicated by arrow 1).[25,26] The amount of moisture released was the same in WG (5.3 ± 0.4 wt %) and WGG (5.2 ± 1.5 wt %). In the second region, observed only for WGG, the plasticizer was eliminated (ca. 180 to 250 °C, arrow 2). The third region involved the cleavage of weaker peptide bonds (from ca. 220 to 450 °C, arrow 3). In WGG, this region partly overlapped the second region (arrow 4). The fourth region (ca. 450 to 600 °C, arrow 5) involved, among others, the cleavage of stronger peptide bonds. In the case of WGG, complete decomposition occurred already at ca. 580 °C, explained by Verbeek. et al.[25] as being due to fewer protein–protein interactions in the presence of the plasticizer. In the case of the unplasticized protein (WG) complete decomposition occurred in the fifth region (between ca. 660 and 760 °C, arrow 6), in agreement with data on unplasticised soy protein.[26] Even though the WG and WGG curves were different, the contents of the final char (10.7 ± 0.7 (WG) wt % and 8.2 ± 1.6 wt % (WGG)) were insignificantly different.

The combustion behavior of the gluten foams was evaluated in a cone calorimeter. The heat released from a material undergoing flaming combustion is considered to be the single

dx.doi.org/10.1021/am2017877 | ACS Appl. Mater. Interfaces 2012, 4, 1629–1635

Table 3. Cone Calorimeter Results[a]

sample	density[b] (kg/m^3)	peak HRR[c] (kW/m^2)	avg HRR[d] (180) (kW/m^2)	ΔH_C[e] (kJ/g)	time to ignition[f] (s)	residual mass[g] (%)
PUR[37]	25 ± 2	289	153	27 ± 1[36]	3	NA
WG	131 ± 6	325 ± 13	172 ± 24	19.1 ± 0.1	18 ± 1	12 ± 1
WGG	140 ± 9	401 ± 57	158 ± 28	17.9 ± 1.2	18 ± 6	10 ± 3

[a]± values are standard deviations. [b]Density of the foam samples measured before the cone calorimeter test. [c]The peak of heat release rate. [d]The average heat release rate after 180 s. [e]The effective heat of combustion. [f]Time to ignition after applying a heat flux of 35 kW/m^3. [g]Residual mass after the cone calorimeter test.

most important parameter that characterizes the fire hazard posed by the material.[27] The cone calorimeter makes it possible to measure the rate of heat release from a sample on a bench scale using oxygen calorimetry.[28,29] Data acquired by this technique are relevant for the well-ventilated, developing stage of a fire. The time to ignition and the peak and average rates of heat release are relevant parameters that are associated with the ignitability,[30] flame-spreading tendency, and resultant fire growth potential of the material.[31−33] The parameters were measured here and are presented in Table 3. Figure 4 shows

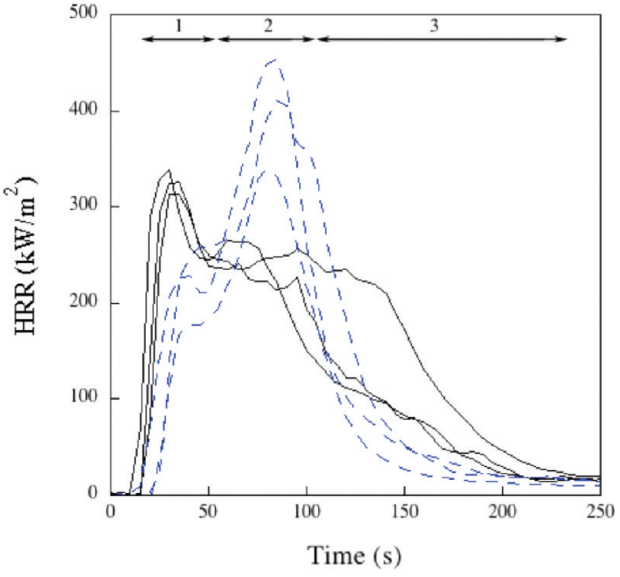

Figure 4. Heat release rate of WG (solid lines) and WGG (broken lines) foams exposed to an incident heat flux of 35 kW/m^2. The locations of stages 1−3 are approximate and varies, as observed, from sample to sample.

that WG and WGG behaved differently during burning. The combustion of the WG sample proceeded in three principal stages (Figures 4 and 5a−c). At first, directly after ignition, the specimen surface was bubbling vigorously for a few seconds. The peak rate of heat release 325 kW/m^2 was attained in the first stage for the WG foam (after 33 s). Shortly after ignition, a char layer formed on the specimen surface and the heat release rate was relatively constant (ca. 220 kW/m^2, stage 2). The char layer on the surface became thicker and expanded slightly. Because it shielded the foam from both heat and oxygen, the size of the flame, and accordingly the heat release rate, decreased at longer times (stage 3), leaving a glowing residue in the sample holder. The combustion of the WGG sample also occurred in three stages, albeit having a different pattern from that of the WG (Figure 4). As in the case of the WG, the WGG foam exhibited vigorous bubbling shortly after ignition (stage 1). However the bubbling of the WGG sample was more vigorous and continued for a longer time. This resulted in higher rates of heat release in the second stage after 180 s; at this stage the peak of the heat release rate of 401 kW/m^2 also occurred. It should be noted that at this stage, a larger flame

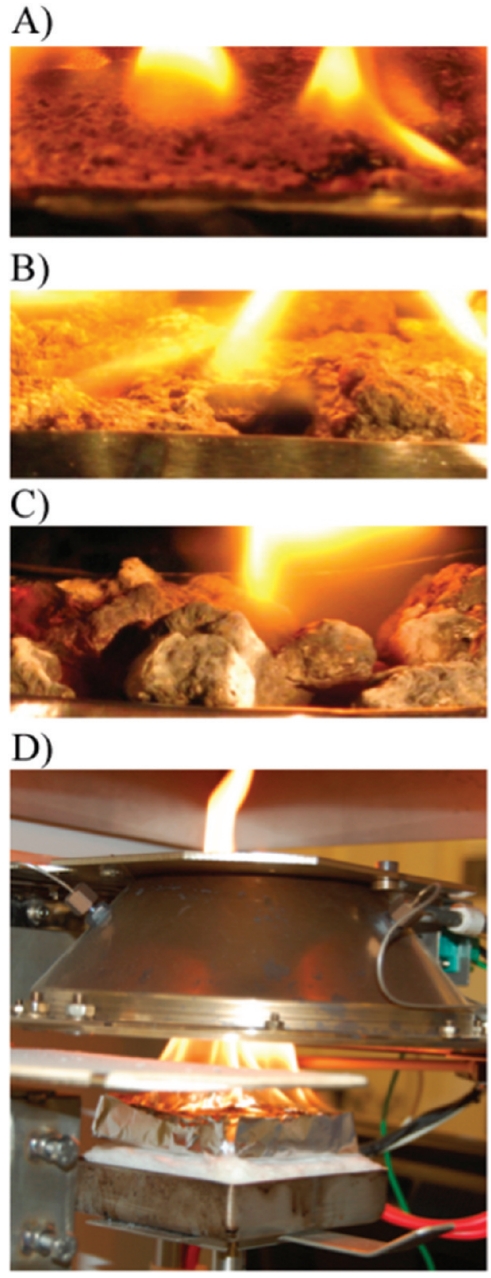

Figure 5. Pictures of the WG foam surface captured at: (A) stage 1, (B) stage 2, and (C) stage 3 of the burning as indicated in Figure 4. (D) Large flame observed during the second stage for the WGG foam.

dx.doi.org/10.1021/am2017877 | ACS Appl. Mater. Interfaces 2012, 4, 1629−1635

(Figure 5d) and an even more vigorous bubbling at the surface were observed. Shortly after the peak of the heat release rate was reached (a few seconds), a char layer formed on the WGG surface (stage 3). This resulted in a reduction in size of the flame and a reduction in the heat release rate, leaving a glowing residual material in the sample holder. Compared to the WG foam, the char formation of the WGG foam came later, which meant that the bubbling persisted for a longer time and that the maximum heat release rate was reached before the surface was charred. It should be noted that the amount of char was somewhat higher than that observed with TGA for both the samples. FE-SEM revealed that the char occurred as a "residual" skeleton structure, resembling the initial pore structure (Figure 6).

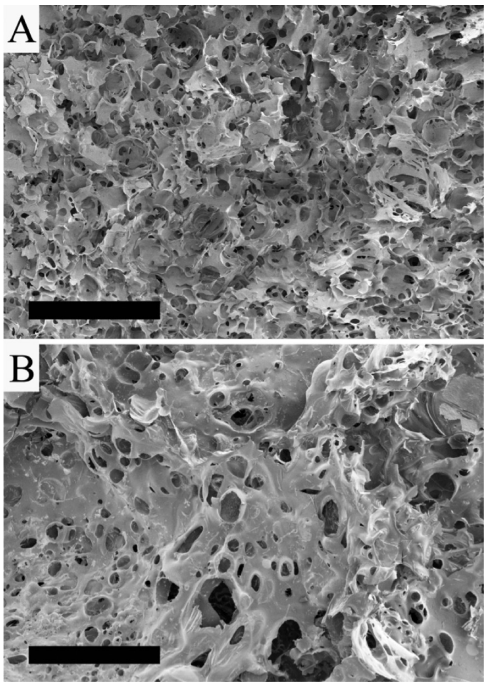

Figure 6. FE-SEM images of the WG foam (a) before and (b) after the cone-calorimeter test. The scale bars are 500 μm long.

Table 3 also includes literature data for a flame-retardant-free polyurethane foam (PUR).[34] It should be kept in mind, though, when comparing polyurethane and wheat gluten data, that they differ in density, air-permeability and thermal properties, and that a structural collapse of polyurethane foams may occur during fire. Nevertheless, the gluten foams showed a significantly longer time to ignition than was observed for the polyurethane foam, a result probably due to the presence of moisture in the former foams. It was also important that, in contrast to polyurethane foams, no low viscous liquid tar was formed during the combustion of either the WG or the WGG foam. A liquid tar can form a pool fire and significantly increase the risk of fire spread, as well as accelerating the foam combustion by creating a feed-back loop.[35−37] Even though the glycerol-containing sample (WGG) showed a long time to ignition and a high char yield, its higher rate of heat release, vigorous bubbling and enhanced flame formation during combustion made it less suitable than WG with respect to fire-proof properties. It should however be pointed out that both WG and WGG had substantially lower effective heats of combustion than the polyurethane sample (Table 3).

The smoke- and gas-release data obtained during the cone calorimeter test are summarized in Table 4. The amount of smoke is usually reported as the specific extinction area (SEA), which is given by the extinction coefficient multiplied by the gas volume flow and divided by the loss of mass of the specimen. SEA was lower for the gluten foams than for the PUR foam. The gluten foams also had a lower peak rate of smoke release (PRSR) than that of the PUR foam. Even though both gluten foams showed lower smoke densities, they emitted significantly more carbon monoxide (CO), whereas the emissions of CO_2 from the gluten foams were comparable to those from PUR. The average rate of mass loss during the cone-calorimeter test (MLR) was approximately the same for all three materials.

On the basis of the findings from the cone-calorimeter test, it was decided to continue and to make the UL94 test on the unplasticised sample (WG) (Table 4). An initial evaluation was also made on a WGG sample, but it was found to burn continuously. Some interesting findings could be drawn directly from the burning test on WG: Although the times varied, the foam self-extinguished when the flame was removed and dripping was absent. Once the specimens were ignited, they burned slowly with a small ca. 10 mm size flame on one side.

According to UL 94, materials are classified in three different groups: V-0, V-1, and V-2. In V-0, the time of burning with flaming combustion (t_1 or t_2) should not exceed 10 s, nor should the total time ($t_1 + t_2$) for five specimens exceed 50 s. In V-1 the corresponding times are 30 and 250 s. V-2 has the same limit of after-flame times as V-1, but, in contrast to V-0 and V-1, cotton ignition caused by material dripping is acceptable here. If a material does not satisfy any of the criteria it fails to be classified according to the UL 94 standard. As shown in Table 5, the WG foam failed to be classified according to the standard as the individual flaming combustion times (t_1 or t_2) and the total flaming combustion time for all five replicates (324 s) exceeded the criteria. These results are not surprising, since the foam was free from any added flame-retardants and we still conclude that the fire-retardant properties of the WG foam are very promising. One reason for the promising fire properties is undoubtedly the presence of moisture in the foam. However, adding more water is not desirable because it may initiate microbial growth. Besides adding a flame-retardant, it may be possible to improve the flame-retardant properties by the addition of an inorganic component (e.g., clay or silica).

Table 4. Smoke and Gas Production in the Cone Calorimeter[a]

sample	PRSR[b] (1/s)	SEA (180)[c] (m^2/kg)	CO (180)[d] (kg/kg)	CO_2 (180)[e] (kg/kg)	MLR (180)[f] (g/s)
PUR[37]	5.5	187	0.008	1.89	0.058
WG	3.9 ± 0.2	179 ± 1	0.020 ± 0.001	1.78 ± 0.16	0.063 ± 0.012
WGG	4.1 ± 0.6	118 ± 10	0.019 ± 0.001	1.77 ± 0.03	0.067 ± 0.002

[a]± values are standard deviations. [b]The average peak rate of smoke release. [c]The average specific extinction area after 180 s. [d]Total CO release after 180 s. [e]Total CO_2 release after 180 s. [f]The average mass loss rate after 180 s.

Table 5. UL 94 Data for WG

	first flame application		second flame application	
sample	flaming combustion time t_1 (s)	drip and cotton ignition	flaming combustion time t_2 (s)	drip and cotton ignition
1	1	no	62	yes[a]
2	34	no	11	no
3	64	no	6	no
4	38	no	24	no
5	76	no	8	no
avg	36 ± 30	no	29 ± 27	no

[a]Piece of material fell off and ignited the cotton.

CONCLUSIONS

The freeze-drying technique yielded wheat gluten foams with only slightly higher thermal conductivities than commercial polystyrene and polyurethane insulation foams, as was also shown previously for freeze-dried clay/casein foams.[23] This was observed despite the fact that the freeze-drying yielded mainly open pores. In fact, the thermal conductivity was similar to that of glass-wool materials.[38] The freeze-dried foams also showed interesting flame-retardant properties, even though they contained no added flame-retarder. Evidently the naturally occurring 5 wt % moisture had a beneficial delaying effect on the cone-calorimeter ignition times. For insulation applications, it was also important that the foams yielded a large char residue rather than a low viscous tar.

AUTHOR INFORMATION

Corresponding Author

*E-mail: mikaelhe@polymer.kth.se. Fax: +4687906030.

Notes

The authors declare no competing financial interest.

ACKNOWLEDGMENTS

We acknowledge Dr. Roland H. Krämer for the assistance with his expertise in the combustion part of the paper.

REFERENCES

(1) Gibson, L. J.; Ahsby, M. F. *Cellular Solids: Structure and Properties*, 2nd ed.; Pergamon: Oxford, 1988.
(2) Alvarez-Lainez, M.; Rodriguez-Perez, M. A.; de Saja, J. A. *J. Polym. Sci.* **2008**, *46*, 212−221.
(3) Almanza, O.; Rodríguez-Pérez, M. A.; de Saja, J. A. *Polym. Int.* **2004**, *53*, 2038−2044.
(4) De Carvalho, G.; Pimenta, J. A.; Dos Santos, W. N.; Frollini, E. *Polym-Plast. Technol.* **2003**, *44* (4), 605−626.
(5) Gautam, R.; Bassi, A. S.; Yanful, E. K. *Appl. Biochem. Biotechnol.* **2007**, *141*, 85−108.
(6) Chao, C. Y. H.; Wang, J. H. *J. Fire Sci.* **2001**, *19*, 137−156.
(7) Ahrens, M., *Home Fires That Began with Upholstered Furniture*. National Fire Protection Association: Quincy, 2008; p 68.
(8) Blomfeldt, T. O. J.; Olsson, R. T.; Menon, M.; Plackett, D.; Johansson, E.; Hedenqvist, M. S. *Macromol. Mater. Eng.* **2010**, *295*, 796−801.
(9) Blomfeldt, T. O. J.; Kuktaite, R.; Johansson, E.; Hedenqvist, M. S. *Biomacromolecules* **2011**, *12*, 1707−1715.
(10) Olabarrieta, I.; Cho, S.-W.; Gällstedt, M.; Sarasua, J.-R.; Johansson, E.; Hedenqvist, M. S. *Biomacromolecules* **2006**, *7*, 1657−1664.
(11) Ullsten, H. N.; Gällstedt, M.; Johansson, E.; Gräslund, A.; Hedenqvist, M. S. *Biomacromolecules* **2006**, *7*, 771−776.
(12) Gällstedt, M.; Mattozzi., A.; Johansson, E.; Hedenqvist, M. S. *Biomacromolecules* **2004**, *5*, 2020−2028.
(13) Min, S.; Blumm, J.; Lindemann, A. *Thermochim. Acta* **2007**, *455*, 46−49.
(14) *ISO 5660−1:2002. Reaction-to-fire tests - Heat release, smoke production and mass loss rate - Part 1: Heat release rate (cone calorimeter method)*; International Organisation of Standardization: Geneva, Switzerland, 2002.
(15) Lim, H.; Kim, S. H.; Kim, B. K. *Express. Polym. Lett.* **2008**, *2*, 194−200.
(16) www.isover.com
(17) Yang, C. G.; Xu, L.; Zhang, L. Q.; Chen, N. *Energy Convers. Manage.* **2006**, *47*, 1124−1132.
(18) Rudtsch, S.; Hammerschmidt, U. *Int. J. Thermophys.* **2004**, *25*, 1475−1582.
(19) Al-Ajlan, S A. *Appl. Therm. Eng.* **2006**, *26*, 2184−2191.
(20) Lim, K.-H.; Kim, S.-K.; Chung, M.-K. *Thermochim. Acta* **2009**, *494*, 71−79.
(21) Prociak, A.; Pielichowski, J.; Sterzynski, T. *Polym. Test.* **2000**, *19*, 705−712.
(22) dos Santos, W. N.; Mummery, P.; Wallwork, A. *Polym. Test.* **2005**, *24*, 628−634.
(23) Gawryla, M. D.; Nezamsadeh, M.; Schiraldi, D. A. *Green Chem.* **2008**, *10*, 1078−1081.
(24) Assael, M. J.; Botsios, S.; Gialou, K.; Metaxa, I. N. *Int. J. Thermophys* **2005**, *26*, 1595−1605.
(25) Verbeek, C. J. R.; van den Berg, L. E. *Macromol. Mater. Eng.* **2010**, *295*, 10−21.
(26) Swain, S. N.; Rao, K. K.; Nayak, P. L. *J. Appl. Polym. Sci.* **2004**, *93*, 2590−2596.
(27) Janssens, M. L. *Fire Technol.* **1991**, *27*, 234.
(28) Babrauskas, V. *Ignition Handbook*; Fire Science Publishers: Issaquah, WA, 2003.
(29) Karlsson, B. A. *Fire Safety J.* **1993**, *20*, 93−113.
(30) Grant, G.; Drysdale, D. *Fire Safety J.* **1995**, *24*, 247−278.
(31) Kuang-Chung, T.; Drysdale, D. *Fire Safety J* **2002**, *37*, 697−706.
(32) Schartel, B.; Hull, T. R. *Fire Mater.* **2007**, *31*, 327−354.
(33) Zhang, J.; Shields, T.; Silcock, G. *Fire Mater.* **1997**, *21*, 1.
(34) Price, D.; Liu, Y.; Hull, R. T.; Milnes, G. J.; Kandola, B. K.; Horrocks, R. A. *Polym. Int.* **2000**, *49*, 1153−1157.
(35) Krämer, R. H.; Zammarano, M.; Linteris, G. T.; Gedde, U. W.; Gilman, J. W. *Polym. Degrad stabil.* **2010**, *95*, 1115−1122.
(36) Ohlemiller, T. J.; Shields, J. R. *NIST Technical Note 1493*; National Institute of Standards and Technology: Gaithersburg, MD, 2008.
(37) Checchin, M.; Cecchini, C.; Cellarosi, B.; Sam, F. O. *Polym. Degrad. Sabil.* **1999**, *64*, 573−576.
(38) Mathias, J.-D.; Tessier-Doyen, N.; Michaud, P. *Int. J. Mol. Sci.* **2011**, *12*, 1175−1186.